Source/Drain Engineering for High-Performance deep sub-100nm Ge-pMOSFETs using Full-Band Monte Carlo Simulation

Hiroshi Takeda[1], Takeo Ikezawa[2], Michihito Kawada[2] and Masami Hane[1]
[1]LSI Fundamental Research Laboratory, NEC Electronics Corporation,
[2]NEC Informatec Systems, Ltd.
1120 Shimokuzawa, Sagamihara, Kanagawa 229-1198, Japan
E-mail: hiroshi.takeda@necel.com

Abstract— **Full-band Monte Carlo simulation was performed to explore the optimal source/drain (SD) structure for deep sub-100nm Ge-pMOSFETs. Comparing the source-to-channel carrier injection characteristics of metal SD and conventional pn-junction SD devices, suitable SD structure for high-performance Ge-devices were discussed. MSD devices outperform pn-SD ones in the "Schottky" SD condition while they exhibit almost the same device characteristics in the "ohmic" SD condition.**

Keywords; Ge, MOSFET, Schottky, metal source/drain, full-band, Monte Carlo

I. INTRODUCTION

High mobility Ge-channel pMOSFETs have been attractive for future high speed and low power CMOS devices. However, the transport characteristics of short-channel devices may not be explained merely by the low-filed mobility. It is, therefore, important to investigate the actual device performance of short-channel Ge-pMOSFETs.

Recently, sub-100nm Ge-pMOSFETs with NiGe metal source/drain (MSD) have been demonstrated [1]. In order to explore the feasibility of the sub-100nm and further scaled MSD Ge-pMOSFETs, we have performed detailed transport analysis for the short-channel MSD Ge-pMOSFETs comparing with MSD Si-pMOSFETs [2]. In [2], we clarified that the improvement of the source-to-channel carrier injection is a key to achieve high-performance sub-100nm MSD Ge-pMOSFETs since the small source-to-channel injected carrier density limits the on-state drain current of Ge-pMOSFETs. In order to improve the source-to-channel carrier injection, Schottky barrier reduction is effective for MSD devices [2].

On the other hand, conventional pn-junction source/drain (pn-SD) structure is also able to improve the source-to-channel carrier injection since the source-to-channel injected carrier density is controlled by the doping concentration in the pn-SD. Thus, it is not clear whether the MSD is the optimal source/drain structure from the aspect of the efficient source-to-channel carrier injection while the MSD structure exhibits very low sheet resistance [1]. In order to address the optimal source/drain structure for further high-performance Ge-pMOSFETs, comparative study would be demanded in terms of the transport properties for the MSD and the pn-SD devices. In this work, we have, therefore, simulated the device characteristics of MSD and pn-SD deep sub-100nm Ge-pMOSFET and made a detailed comparison of their carrier transport properties using full-band Monte Carlo device simulation.

II. CALCULATION METHOD

Our full-band Monte Carlo device simulator [3] takes into account quantization effects along the gate confinement direction with the full-band structure calculated by an empirical pseudo potential method. Phonon and surface roughness scattering effects are included in our simulation. Surface roughness parameters [4] are adjusted to reproduce the experimental inversion layer hole mobility of [1], and the bulk-phonon parameters [5] are used for phonon scattering.

For the channel carrier injection from MSD, we consider tunneling carrier injection through the Schottky barrier at the MSD/channel interface in addition to the thermal carrier injection from the thermal equilibrium MSD. Thermally injected carrier density at the MSD/channel interface, $N_{S/D}^{Thermal}$, is calculated as follows:

$$N_{\mathrm{S/D}}^{\mathrm{thermal}} = \int_{-\infty}^{\infty} D_{\mathrm{S/D}}(E) f_{\mathrm{S/D}}(E) dE. \qquad (1)$$

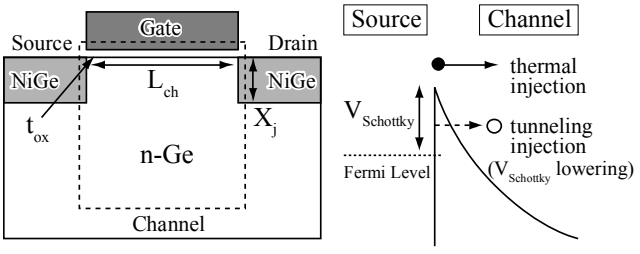

Figure 1. Ge-pMOSFET with NiGe metal source/drain (MSD) [1]. t_{ox} and X_j represent effective oxide thickness and MSD layer depth, respectively. Substrate doping density is $N_{sub} = 3.3 \times 10^{17}$ cm^{-3}. Schottky barrier height $V_{Schottky} = 60$ meV for NiGe/n-Ge. Carrier tunneling injection is taken into account through the $V_{Schottky}$ lowering.

978-1-4244-1753-7/08/$25.00 ©2008 IEEE

$D_{S/D}$ indicates a local density of states at the MSD/channel interface, and $f_{S/D}$ is a Fermi distribution function of MSD. $D_{S/D}$ is obtained by a calculated quantized band structure, and carriers having positive (negative) velocity along the source-drain direction can be thermally injected into the channel from the metal source (drain) as shown in Fig. 1. On the other hand, tunneling injected carrier density, N_{SD}^{tunnel} is calculated as

$$N_{S/D}^{tunnel} = \int_{-\infty}^{E_0} D_{S/D}(E_0) T_{S/D}(E) f_{S/D}(E) dE, \quad (2)$$

where E_0 is the minimum energy of the first subband and $T_{S/D}$ is a tunneling probability of Schottky barrier which, in this work, is calculated based on the WKB approximation. Since our device simulator is based on the classical carrier transport, tunneling carrier injection is treated as a Schottky barrier ($V_{Schottky}$) lowering as shown in Fig. 1. The magnitude of the Schottky barrier lowering, $\Delta V_{Schottky}$, is determined to match the thermally injected carrier density with the Schottky barrier lowering to the net (thermally and tunneling) injected carrier density, namely,

$$N_{S/D} = N_{S/D}^{thermal} + N_{S/D}^{tunnel} = \int_{-\infty}^{\infty} D_{S/D}(E - \Delta V_{Schottky}) f_{S/D}(E) dE. \quad (3)$$

Considering the tunneling carrier injection in addition to the surface roughness parameters adjustment, our device simulator can well reproduce experimental I_d-V_g and I_d-V_d curves of fabricated NiGe MSD ($V_{Schottky}$ = 60 meV) Ge-pMOSFET with L_{ch} = 80 nm [1] as shown in Fig. 2. Since any leakage current components are not included in our simulation, the calculated results for example in the sub-threshold or saturation regions differ from the experimental ones. In this paper, the ideal device characteristics without the leakage current is discussed for both MSD and pn-SD devices.

For conventional pn-SD devices, carrier density in the source/drain regions are determined by the doping concentration of pn-SD, N_{pn}, and the channel injected carrier density is controlled by the channel bottleneck point.

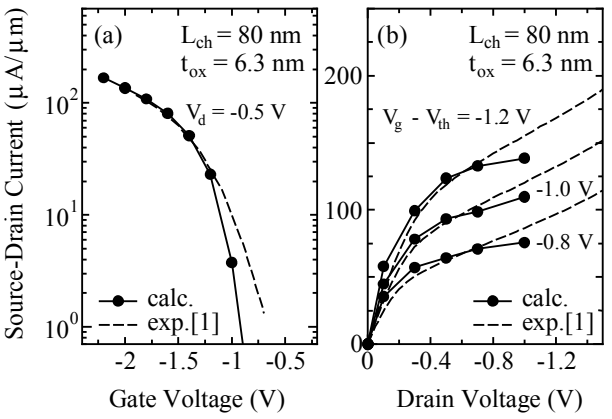

Figure 2. (a) I_d-V_g and (b) I_d-V_d characteristics of L_{ch} = 80 nm MSD Ge-pMOSFET with N_{sub} = 3.3x10^{17} cm^{-3} channel. Experimental results [1] show significant leakage current especially in sub-threshold region.

III. Comparative Analysis between MSD and pn-SD

For further scaled situations, L_{ch} = 30 nm MSD and pn-SD Ge-pMOSFETs with t_{ox} = 2 nm gate oxide are simulated in this work. Substrate doping concentration, N_{sub}, is set to be 3.3x10^{17} cm^{-3}. $V_{Schottky}$ and N_{pn} are changed for MSD and pn-SD devices, respectively. In the following subsections, we will compare the device characteristics of MSD and pn-SD devices with the same off-state source/drain (SD) carrier density conditions.

A. Comparison with NiGe MSD Ge-pMOSFETs

First, we compare the device characteristics of fabricated NiGe MSD ($V_{Schottky}$ = 60 meV) Ge-pMOSFETs [1] to those of the pn-SD ones with the same off-state SD carrier density condition. Fig. 3 shows I_d-V_g characteristics of NiGe MSD and pn-SD (N_{pn} = 1.7x10^{18} cm^{-3}) devices. Under the same off-state SD carrier density condition, the MSD device shows higher on-current than in the pn-SD device since the carrier density at the source/channel interface of the MSD device increases with $|V_g|$ in contrast to the pn-SD case as seen in Fig. 4. This is due to the additional tunneling carrier injection through the source/channel Schottky barrier in the MSD device, which is increased by the strong lateral electric filed at the on-state (Fig. 5). The tunneling injected carrier density reaches to about 85% of the net channel injected carrier density of the MSD device at the on-state, and this higher carrier density results in the higher on-state drain current in the MSD devices.

On the other hand, at the off-state, the tunneling carrier injection is negligible due to the off-state channel barrier, so that the same source/drain carrier density is obtained both in the MSD and pn-SD devices (Fig. 4). Since the channel potential is fixed at the MSD interfaces of the MSD devices, the off-state channel barrier potential is rather lower and thinner compared to the pn-SD devices. As a result, the off-state current is a little higher than that of the pn-SD devices where the channel potential gradually varies around the pn-SD/channel interfaces. However, the effects of the higher channel injected carrier density at the on-state are more significant for the device characteristics. Thus, the MSD devices outperform the pn-SD ones in such low SD carrier density conditions.

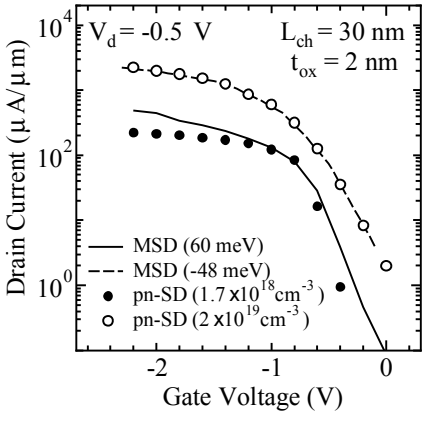

Figure 3. I_d-V_g characteristics of MSD and pn-SD devices. pn-SD (N_{pn} = 1.7x10^{18} cm^{-3}) has the same SD carrier density of NiGe MSD ($V_{Schottky}$ = 60 meV). MSD ($V_{Schottky}$ = -48 meV) and pn-SD (N_{pn} = 2x10^{19} cm^{-3}) are regarded as ohmic SD devices.

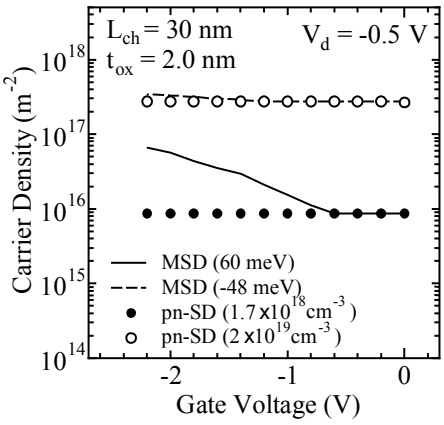

Figure 4. Carrier density at the source/ channel interface of MSD device and that in the source region of pn-SD device. MSD devices show larger carrier density at the on-state due to carrier tunneling injection from source to channel.

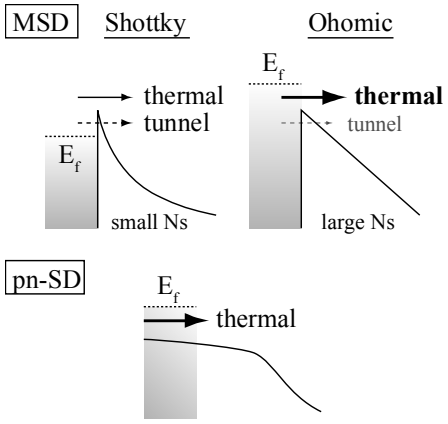

Figure 5. Tunneling carriers are more significant in Schottky MSD ($V_{Schottky} > 0$) device. Thermal carrier component is dominant for transport characteristics in ohmic MSD device ($V_{Schottky} < 0$) as in pn-SD devices.

B. Ohomic SD Condition Devices

In order to enhance the on-current of MSD devices, it is required to lower $V_{Schottky}$ and improve the carrier injection from MSD into the channel [2]. Ideally, $V_{Schottky}$ is desirable to be zero or negative for high-performance devices. As an example of such "ohmic" MSD ($V_{Schottky} < 0$) devices, I_d-V_g characteristics of $V_{Schottky}$ = -48 meV MSD device is also plotted in Fig. 3, in addition to that of the corresponding $N_{pn} = 2x10^{19}$ cm^{-3} pn-SD device having the same off-state SD carrier density.

Under the ohmic SD condition, the pn-SD device shows almost the same I_d-V_g characteristics as in the MSD device. Thus, if sufficiently high SD carrier density is achieved, both "ohmic" MSD and highly doped pn-SD structures can be applied for high-performance devices. In this case, the SD carrier density of MSD devices is independent of V_g as seen in Fig. 4 since thermal carrier injection dominates the transport characteristics. Due to the sufficiently high Fermi level in MSD and somewhat suppressed longitudinal electric filed by the high channel injected carrier density, thermally injected carrier density component is much larger than the tunneling injected one even at the on-state in the "ohmic" MSD devices (Fig. 5). The sub-threshold characteristics of the MSD and pn-SD devices are also comparable, while the higher Fermi level in the SD regions of "ohmic" SD devices causes the threshold voltage lowering compared to the "Schottky" MSD device with $V_{Schottky}$ = 60 meV.

Since the thermally injected carriers dominate the transport characteristics of the "ohmic" MSD device, the V_g dependency of the carrier velocity at the source/channel interface is about the same as that of the carrier velocity in the source region of the pn-SD device (Fig. 6). With such the same transport characteristics, both the MSD and the pn-SD devices show the same device characteristics in the ohmic SD conditions.

IV. Carrier Velocity Characteristics

Compared to the "Schottky" MSD ($V_{Schottky} > 0$) devices, the "ohmic" MSD ($V_{Schottky} < 0$) ones tend to show the lower carrier velocity across the source/channel interface (Fig. 6). Since the higher average energy of the channel injected carriers in the "ohmic" MSD device with the higher Fermi level of the MSD results in the higher scattering rate around the source/channel interface, the channel backscattering indicator (current ratio of the backward current to the forward current, $I_{back} / I_{forward}$) is larger in the "ohmic" MSD ($V_{Schottky}$ = -48 meV) device than in the "Schottky" MSD ($V_{Schottky}$ = 60 meV) one with the same lateral electric filed at the source/channel interface (Fig. 7). Thus, the rectification nature of the MSD with strong lateral electric field at the source/channel interface becomes weak as $V_{Schottky}$ is lowered, and the carrier velocity is lower in the "ohmic" device although the injection velocity, v_{inj}, is about 15% higher in the "ohmic" MSD device (v_{inj} = $1.07x10^7$ cm/sec) than in the "Schottky" MSD device (v_{inj} = $0.92x10^7$ cm/sec) because of the higher carrier energy.

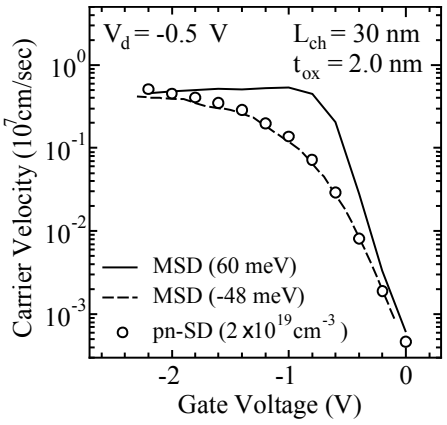

Figure 6. V_g dependence of carrier velocity at the source/channel interface of MSD device. Ohmic MSD device ($V_{Schottky} < 0$) has similar carrier velocity as in the source region of pn-SD device with the same SD carrier density.

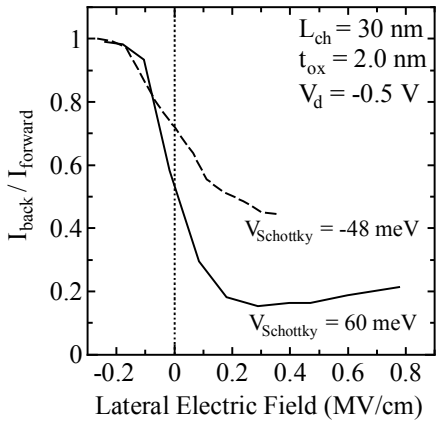

Figure 7. Current ratio of I_{back} to $I_{forward}$ at the source/channel interface of MSD device as a backscattering indicator. $I_{forward}$ and I_{back} indicate source-to-drain and drain-to-source current, respectively. I_{back} / $I_{forward}$ becomes larger in ohmic MSD with higher carrier energy due to phonon emission scattering process.

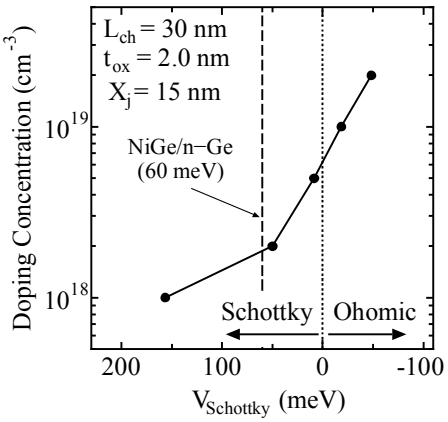

Figure 8. Doping density of pn-SD (N_{pn}) having the same SD carrier density as in the MSD with a Schottky barrier height ($V_{Schottky}$). Depth of MSD and pn-SD (X_j) is set to be 15 nm. Device characteristics of MSD and pn-SD device are similar in the Ohmic region ($V_{Schottky} < 0$) but in the Schottky region ($V_{Schottky} > 0$).

However, at the on-state, strong longitudinal electric field leads to sufficiently small back-scattering rate even in the "ohmic" MSD device, and the back-scattering rate in the "Schottky" MSD device is saturated by the $V_{Schottky}$ lowering with significant tunneling carrier injection. In addition to the higher v_{inj}, this sufficiently small back-scattering rate results in the comparable net carrier velocity across the source/channel interface in the "ohmic" MSD device to the "Schottky" MSD devices at the on-state. The on-state drain current of the "ohmic" MSD devices, thereby, exceeds that of the "Schottky" MSD devices due to much higher channel injected carrier density.

V. Relation between $V_{Schottky}$ and N_{pn}

Fig. 8 shows the N_{pn}-$V_{Schottky}$ relation with the same off-state SD carrier density for MSD and pn-SD L_{ch} = 30 nm Ge-pMOSFETs. For deep sub-100 nm Ge-pMOSFETs, at least $N_{pn} > 2x10^{18}$ cm^{-3} is required for the pn-SD devices to outperform actually fabricated NiGe MSD devices ($V_{Schottky}$ = 60 meV) because of the higher on-current in the MSD devices under the same off-state SD carrier density condition. If $N_{pn} > 2x10^{18}$ cm^{-3} pn-SD with an abrupt doping profile can hardly be obtained, the NiGe MSD is preferable for short-channel Ge-pMOSFETs.

For further high-performance devices, "ohmic" MSD ($V_{Schottky} < 0$) or corresponding highly doped pn-SD ($N_{pn} > 1x10^{19}$ cm^{-3}) is required (Fig. 8). Since, in the ohmic SD region, both MSD and pn-SD devices show almost the same transport characteristics under the same off-state SD carrier density condition, the optimal SD structure depends on the difficulty for the ideal "ohmic" MSD ($V_{Schottky} < 0$) or sufficiently high N_{pn} ($>1x10^{19}$ cm^{-3}) abrupt pn-SD, while both the ohmic SD structures are challenging for short-channel Ge-devices due to the strong Fermi level pinning [6] and the low solid solubility of dopants [7] in Ge-substrate.

VI. Conclusions

We have investigated suitable source/drain structures for high-performance deep sub-100nm Ge-pMOSFETs using full-band Monte Carlo device simulator. The accuracy of our device simulator has been confirmed by reproducing the experimental device characteristics of fabricated sub-100nm NiGe MSD Ge-pMOSFETs.

With the same off-state source/drain carrier density condition, the NiGe MSD ($V_{Schottky}$ = 60 meV) devices with L_{ch} = 30 nm outperform the corresponding pn-SD ($N_{pn} \sim 2x10^{18}$ cm^{-3}) ones because of the additional tunneling carrier injection from source to channel at the on-state. The NiGe MSD devices are, therefore, preferable for deep sub-100nm Ge-pMOSFETs, if $N_{pn} > 2x10^{18}$ cm^{-3} pn-SD with an abrupt doping profile can hardly be obtained.

On the other hand, for further high-performance devices with "ohmic" SD structure, the optimal SD structure depends on the difficulty for ideal "ohmic" MSD ($V_{Schottky} < 0$) or sufficiently high N_{pn} ($> 1x10^{19}$ cm^{-3}) abrupt pn-SD, since both MSD and pn-SD devices show almost the same transport characteristics under the same off-state SD carrier condition.

[1] T. Yamamoto *et al*., IEDM Tech. Dig., 1041 (2007).

[2] H. Takeda, T. Yamamoto, T. Ikezawa, M. Kawada, S. Takagi, and M. Hane, Symp. VLSI Tech. Dig., 58 (2008).

[3] H. Takeda, T. Ikezawa, M. Kawada, and M. Hane, Proc. of SISPAD, 25 (2007).

[4] T. Ando, A.B. Fowler, and F. Stern, Rev. Mod. Phys. **54**, 437 (1982).

[5] M.V. Fischetti and S.E. Laux, J. Appl. Phys. **80**, 2234 (1996).

[6] A. Dimoulas, P. Tsipas, A. Sotiropoulos, and E.K. Evangelou, Appl. Phys. Lett. **89**, 252110 (2006).

[7] S. Uppal et al., J. Appl. Phys. **90**, 4293 (2001).